

DYNAMICAL CLUSTER-DECAY MODEL BASED ON  
SKYRME FORCE KDE0(v1) AND THE DYNAMICS  
OF  $^{208,206,204}\text{Pb} + ^{48}\text{Ca} \rightarrow ^{256,254,252}\text{No}^*$  REACTION\*

NIYTI, RAJPAL SINGH

Gandhi Memorial National College, Ambala Cantt., Haryana-133001, India

AMAN DEEP, RAJESH KHARAB

Department of Physics, Kurukshetra University, Kurukshetra-136119, India

SAHILA CHOPRA, RAJ K. GUPTA

Department of Physics, Panjab University, Chandigarh-160014, India

*(Received January 12, 2018)*

Extending our earlier work on  $^{48}\text{Ca} + ^{204,206,208}\text{Pb}$  reactions, based on the Dynamical Cluster-decay Model (DCM) using the pocket formula for nuclear proximity potential, we study the cross sections  $\sigma_{xn}$  for the decay of the compound nuclei  $^{252,254,256}\text{No}^*$ , synthesized in  $^{48}\text{Ca} + ^{204,206,208}\text{Pb}$  fusion reactions, via  $1n$ - $4n$  evaporation channels. For this study, we use the DCM with the Skyrme force KDE0(v1). Deformations  $\beta_{2i}$  and hot-optimum orientations  $\theta_i$  at various excitation energies  $E^*$  from 19.6 to 43.6 MeV are included. Interestingly, for the use of a Skyrme force, the DCM reproduces the data very well with one parameter  $\Delta R$  fitted to the measured data on fusion evaporation residues (ER).

DOI:10.5506/APhysPolB.49.639

## 1. Introduction

The  $\text{Pb} + ^{48}\text{Ca}$  reactions have been experimentally studied since 1975, at various compound nucleus (CN) excitation energies  $E^*$ . We base our study on the experimental data of Ref. [1], where the  $2n$  emission channel was observed for  $^{204,206,208}\text{Pb} + ^{48}\text{Ca}$  reactions at  $E^* = 20$ – $45$  MeV, and the  $1n$ ,  $3n$  and  $4n$  emission channels were measured only for the  $^{206}\text{Pb} + ^{48}\text{Ca}$

---

\* Presented at the XXXV Mazurian Lakes Conference on Physics, Piaski, Poland, September 3–9, 2017.

reaction at some excitation energies. In Ref. [2], the dynamical cluster-decay model (DCM), using a pocket formula for the nuclear proximity potential was shown to give a good description of the measured individual channels with emission of light particles (here: neutrons) for configurations of “hot, compact” orientations  $\theta_{ci}$  (where  $c$  stands for compact and  $i = 1, 2$  for two nuclei/fragments), with only one parameter (neck length  $\Delta R$ ) fitted. In the present work, we would like to analyze the role of other nuclear interaction potentials, namely, those derived from the Skyrme energy density formalism (SEDF) based on the semiclassical extended Thomas Fermi method (ETF) under frozen density approximation [3], in addition to the pocket formula used in Ref. [2].

We choose the KDE0(v1) Skyrme force [4], and compare the obtained results with our earlier calculations [2] based on the proximity potential proposed by Blocki *et al.* We find that KDE0(v1) reproduces well the data for  $1n-4n$  decays of  $^{252,254,256}\text{No}^*$ . Thus, the aim of this paper is to analyze the reaction dynamics, *i.e.*, the decay of  $^{252,254,256}\text{No}^*$ , by reproducing the measured excitation functions for  $1n-4n$  emission (the evaporation residue cross sections  $\sigma_{\text{ER}} = \sum_{x=1}^4 \sigma_{xn}$ ,  $x = 1-4$ , as a function of CN excitation energy  $E^*$ ) using the DCM with Skyrme force KDE0(v1) in terms of a single parameter of the model, the neck-length parameter  $\Delta R$ .

## 2. Methodology

The energy density formalism defines the nuclear interaction potential  $V_{\text{N}}(R)$  *i.e.*, the nucleus-nucleus interaction potential as a function of separation distance

$$V_{\text{N}}(R) = E(R) - E(\infty), \quad (1)$$

*i.e.*, the difference of the expectation value of the energy  $E$  of the colliding nuclei that are overlapping (at a finite separation distance  $R$ ) and that are completely separated (at  $R = \infty$ ), where

$$E = \int H(\vec{r}) d\vec{r}$$

with the Skyrme Hamiltonian density  $H(\rho_i, \tau_i, \vec{J}_i)$  given in terms of the nucleon, kinetic and spin orbit energy densities, as  $\rho = \rho_n + \rho_p$ ,  $\tau = \tau_n + \tau_p$ , and  $\vec{J} = \vec{J}_n + \vec{J}_p$ , respectively [4].

The radius for an axially symmetric deformed nucleus is expressed as

$$R_i(\alpha_i, T) = R_{0i}(T) \left[ 1 + \sum_{\lambda} \beta_{\lambda i} Y_{\lambda}^{(0)}(\alpha_i) \right], \quad (2)$$

with  $R_{0i}$  being the spherical (or, equivalently, the half-density) nuclear radius and  $\alpha_i$  ( $i = 1, 2$ ) being angles between the radius vector  $R_i$  and the nuclear symmetry axis, measured clockwise from the symmetry axis, see Fig. 1 of Ref. [5]. The dependence on the temperature  $T$  is then introduced as in Ref. [6]

$$R_{0i}(T) = R_{0i}(T = 0) (1 + 0.0005T^2), \quad (3)$$

where  $T$  is related to the incoming center-of-mass energy  $E_{\text{cm}}$ , or the CN excitation energy  $E^*$ , via the entrance channel  $Q_{\text{in}}$ -value, following

$$E^* = E_{\text{cm}} + Q_{\text{in}} = \frac{1}{a}AT^2 - T \quad (T \text{ in MeV}) \quad (4)$$

with the empirically fitted constant  $a = 9$  for intermediate-mass nuclei, and  $a = 10$  for super-heavy nuclei.

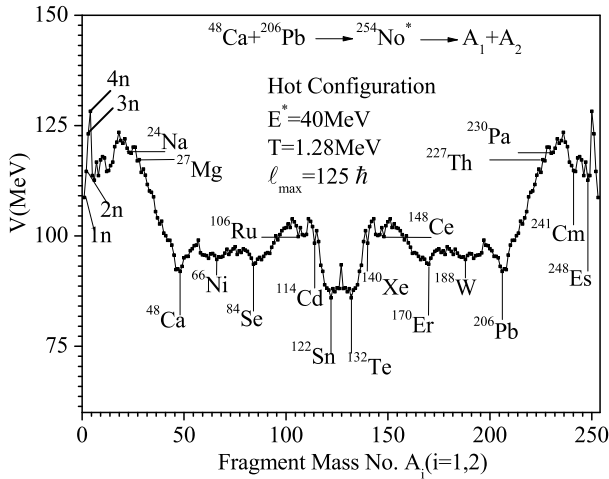


Fig. 1. Mass fragmentation potential  $V(A_i)$ ,  $i = 1, 2$ , at  $\ell = \ell_{\text{max}}$  for the formation of  $^{254}\text{No}^*$  at  $T = 1.28$  MeV (corresponding to  $E^* = 40$  MeV), calculated at  $R = R_t + \Delta R$  with  $\Delta R = 1.0, 1.469, 2.002,$  and  $2.08$  fm for light fragment masses  $A_2 = 1-4$  and  $1.0$  fm for  $5-127$  (and the same for the complementary heavy fragments), providing the best fit to the available data for  $1n-4n$  emission from  $^{254}\text{No}^*$  formed in  $^{48}\text{Ca} + ^{206}\text{Pb}$  reaction, see Fig. 2 (b).

The DCM [2, 7, 8] is worked out in terms of collective coordinates of mass and charge asymmetry  $\eta = (A_1 - A_2)/(A_1 + A_2)$ , and  $\eta_Z = (Z_1 - Z_2)/(Z_1 + Z_2)$ , as well as the relative separation  $R$ , the multipole deformations  $\beta_{\lambda_i}$  and orientations  $\theta_i$  ( $i = 1, 2$ ) of the two nuclei in the same plane. In DCM, we define the compound nucleus decay cross section in terms of  $\ell$  partial waves as

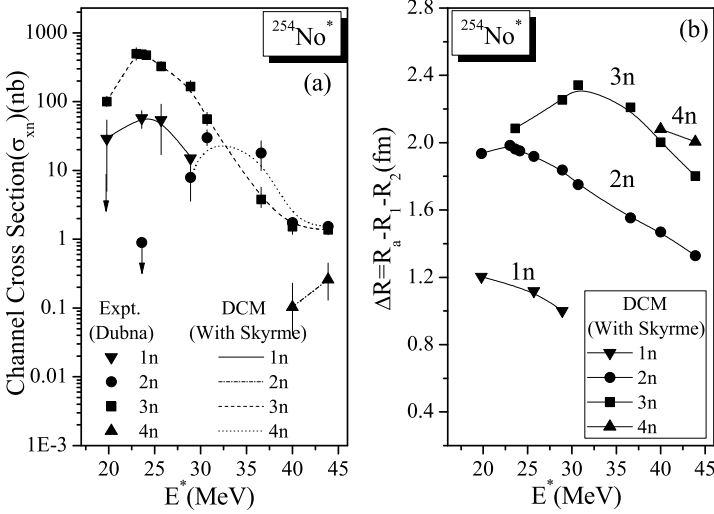


Fig. 2. (a) Excitation functions for individual  $1n$ ,  $2n$ ,  $3n$  and  $4n$  evaporation channels for the  $^{48}\text{Ca}+^{206}\text{Pb}$  reaction in “hot fusion” process. The experimental data is from Ref. [1] (symbols) and the solid lines represent our calculation using DCM with KDE0(v1) Skyrme force, with fitted  $\Delta R$  values presented in Fig. 2(b) as a function of  $E^*$  for neutron evaporation residues from  $^{254}\text{No}^*$  formed in reaction  $^{48}\text{Ca}+^{206}\text{Pb}$ .

$$\sigma = \sum_{\ell=0}^{\ell_{\max}} \sigma_{\ell} = \frac{\pi}{k^2} \sum_{\ell=0}^{\ell_{\max}} (2\ell + 1) P_0^{\ell} P_{\ell}; \quad k = \sqrt{\frac{2\mu E_{\text{cm}}}{\hbar^2}}, \quad (5)$$

where, for each  $\ell$ , the preformation probability  $P_0^{\ell}$  refers to the variation in  $\eta$  ( $\eta$ -motion) and the penetrability  $P_{\ell}$  to  $R$ -motion.  $\ell_{\max}$  is the maximum angular momentum, corresponding to  $\sigma_{\text{ER}}(\ell) \rightarrow 0$ .

### 3. Results and discussion

First of all, we calculate the mass fragmentation potential for all target–projectile combinations ( $A_1$ ,  $A_2$ ) leading to a given compound system formed in  $\text{Pb}+^{48}\text{Ca}$  reactions, as illustrated in Fig. 1 for the case of  $^{48}\text{Ca}+^{206}\text{Pb} \rightarrow ^{254}\text{No}^*$  at  $\ell_{\max} = 125 \hbar$ . The parameter  $\Delta R$  is chosen to provide the best fit to the available data for  $1n$ – $4n$  emission, and at an arbitrary value for heavier ( $A_2 > 4$ ) mass fragments.

Figure 2(a) shows the excitation functions for decay channels  $1n$ – $4n$  from  $^{254}\text{No}^*$  CN formed in  $^{48}\text{Ca}+^{206}\text{Pb}$  reaction. Apparently, independent of the interaction potential used, our calculations with only one parameter  $\Delta R$  are in agreement with experimental results. The calculations are made by

varying a single parameter, the neck length  $\Delta R$ , to obtain the best fit to each measured cross section in each  $xn$  ( $x = 1-4$ ) emission channel. The values of  $\Delta R$  plotted in Fig. 2 (b) show that  $4n$  emission occurs first, followed by  $3n$ , then  $2n$  and finally the  $1n$  emission (smallest  $\Delta R$ ). Clearly, a different  $\Delta R$  for each  $n$ -decay channel means that  $1n-4n$  emission occur in different reaction time scales. For a comparative study of the dependence of cross sections on Pb isotopes used as targets (the isospin ( $N/Z$ ) effect) on nuclear dynamics, we studied the variation of  $\Delta R$  with mass number of compound systems  $^{252,254,256}\text{No}^*$  due to  $^{204,206,208}\text{Pb}+^{48}\text{Ca}$  reactions. We present our results for  $2n$  decay cross sections  $\sigma_{2n}$  in Table I. First, we observe that  $\Delta R_{2n}$  values for the KDE0(v1) Skyrme force are systematically larger than for the nuclear proximity potential of Blocki *et al.* used in our previous work [2]. This happens because the barrier for the nuclear proximity potential lies lower than that for the KDE0(v1) Skyrme force and hence the parameter  $\Delta R_{2n}$  for KDE0(v1) must be larger for a fit to the same  $\sigma_{2n}$  data (see Fig. 3 in Ref. [9]). Secondly, we observe that the cross section for the compound system  $^{256}\text{No}^*$  is the highest and that for  $^{252}\text{No}^*$  is the lowest, with that for  $^{254}\text{No}^*$  lying in between, a result related to the doubly-magic character of both the target ( $^{208}\text{Pb}$ ) and projectile ( $^{48}\text{Ca}$ ) nuclei. The calculations for  $^{207}\text{Pb}^*+^{48}\text{Ca}$  are underway.

TABLE I

Comparison of our present calculation, the earlier work [2], and experimental data of  $2n$ -emission cross sections  $\sigma_{2n}$  from the  $^{252,254,256}\text{No}^*$  CN. The experimental data is from Ref. [1], and the values of the neck-length parameter  $\Delta R_{2n}(E^*)$  for each calculation are also presented in Fig. 2 (b).

Reactions	CN	$E^*$ [MeV]	$T$ [MeV]	$\Delta R_{2n}$ [fm]		$\sigma_{2n}^{\text{Cal}}$ [nb]		$\sigma_{2n}^{\text{Expt}}$ [nb]
				[2]	This work	[2]	This work	
$^{48}\text{Ca}+^{208}\text{Pb}$	$^{256}\text{No}^*$	19.6	0.89	1.953	2.118	1830	1880	1870
		22.3	0.95	1.965	2.098	2050	2050	2050
		24.4	1.0	1.878	2.019	1230	1190	1190
$^{48}\text{Ca}+^{206}\text{Pb}$	$^{254}\text{No}^*$	19.8	0.90	1.816	1.935	106	101	100
		23	0.97	1.833	1.984	495	502	500
		23.6	0.98	1.707	1.963	489	490	489
$^{48}\text{Ca}+^{204}\text{Pb}$	$^{252}\text{No}^*$	20.6	0.92	1.489	1.709	3.49	3.42	3.4
		23.2	0.98	1.605	1.738	15.9	13.2	13.2
		25.4	1.02	1.575	1.718	9.76	9.64	9.6

#### 4. Summary and conclusions

The calculations, using DCM with the KDE0(v1) nuclear interaction potential, were made for the decay of CN  $^{254}\text{No}^*$  formed in the  $^{48}\text{Ca} + ^{206}\text{Pb}$  reaction at various energies ( $E^* = 19.6$  to  $43.6$  MeV), and the results were compared with experiments and our earlier work [2]. The fusion excitation functions of “optimum hot” fusion reactions  $^{48}\text{Ca} + ^{204,206,208}\text{Pb}$  are calculated and reproduce the data well, with one parameter, *i.e.* neck-length  $\Delta R$  fitted. Note that the neck-length parameter is different for each decay channel (here,  $1n-4n$ ), and hence these decays occur in different time scales, *i.e.* with different velocities. Furthermore, since  $\Delta R$ s for the two forces are different, their time scales (equivalently, velocities) are different. Finally, the result of the compound system  $^{256}\text{No}^*$  having the highest cross section is related to the doubly-magic character of both the target ( $^{208}\text{Pb}$ ) and projectile ( $^{48}\text{Ca}$ ) nuclei.

Work supported by the University Grant Commission, Government of India under UGC Rajiv Gandhi National Fellowship (RGNF).

#### REFERENCES

- [1] Yu.T. Oganessian *et al.*, *Phys. Rev. C* **64**, 054606 (2001).
- [2] Niyti, R.K. Gupta, P.O. Hess, *Nucl. Phys. A* **938**, 22 (2015).
- [3] R.K. Gupta, D. Singh, R. Kumar, W. Greiner, *J. Phys. G: Nucl. Part. Phys.* **36**, 075104 (2009).
- [4] B.K. Agrawal *et al.*, *Phys. Rev. C* **73**, 034319 (2006).
- [5] Niyti *et al.*, *Phys. Rev. C* **95**, 034602 (2017).
- [6] S. Shlomo, J.B. Natowitz, *Phys. Rev. C* **44**, 2878 (1991).
- [7] Niyti, R.K. Gupta, *Phys. Rev. C* **89**, 014603 (2014).
- [8] R.K. Gupta, in: *Lecture Notes in Physics*, Vol. 1, *Clusters in Nuclei*, (ed.) C. Beck, Springer-Verlag, Berlin, Heidelberg, 2010, pp. 223–264, DOI:10.1007/978-3-642-13899-7\_6.
- [9] A. Kaur, S. Chopra, R.K. Gupta, *Phys. Rev. C* **91**, 064601 (2015).